ELSEVIER

Composite Structures 47 (1999) 563–569

COMPOSITE STRUCTURES

www.elsevier.com/locate/compstruct

External failure pressure of a frangible laminated composite canister cover

T.Y. Kam *, J.H. Wu, W.T. Wang

Department of Mechanical Engineering, National Chiao Tung University, Hsin-Chu 30050, Taiwan, ROC

Abstract

The static failure strength of a frangible laminated composite canister cover subjected to uniform external pressure is studied via both theoretical and experimental approaches. The frangible canister cover, which is fabricated with four plate-like laminated composite parts, which is designed in such a way that it will fail in a predetermined pattern when subjected to an impulsive internal pressure and its external failure pressure is much higher than its internal failure pressure. The stress distribution in the canister cover is determined using the finite element method and the failure of the cover identified on the basis of an appropriate failure criterion. A number of laminated composite canister covers were fabricated and subjected to static external pressure testing. The failure modes of the frangible covers are studied and the experimental results are used to verify the theoretical predictions. Close agreements between the experimental and theoretical results have been observed. The present study shows that the design of frangible covers with external failure pressure much higher than the internal failure pressure can be achieved. © 2000 Elsevier Science Ltd. All rights reserved.

Keywords: Laminated composite materials; Finite element method; Failure analysis; Frangible cover; Structure; Failure criterion

1. Introduction

The functions of a canister cover are to prevent the leaking out of the inert gas stored in a canister and protect the encanistered missile from attack by foreign objects. In the past, different types of canister covers have been designed and fabricated [1–6]. For instance, canister cover through which missiles exit from missile launchers have used rigid doors or covers that are ruptured by explosive means prior to missile launch. Recently, laminated composite materials have been used in the fabrication of canister covers. For instance, Doane [6] has designed a frangible fly through diaphragm for missile launch canisters using glass/epoxy laminae. The composite canister diaphragm was designed to fail in a predetermined pattern when impacted by the missile nose cone during launch. The disadvantage of this type cover is that it may damage the surface of the missile during the fly through process. Recently, Wu et al. [7] have developed a laminated composite frangible cover, which will not cause any damage on the missile during the fly through process. The special feature of the cover is that it will burst open in accordance with a predetermined pattern and let the encanistered missile fly out of the canister unharmedly when subjected to an internal impulsive pressure generated by the missile engine. Some preliminary results on the static internal failure pressure of the frangible cover have been reported in the literature [7]. In general, canister covers are used for a cluster of canisters. Therefore, the previously proposed frangible cover must also be able to sustain the thrust pressure induced by neighboring missiles during after launch. To ensure no failure occurs, the external failure pressure of the frangible cover must be properly determined.

In this paper, results on the external pressure resistance of the previously proposed frangible cover are presented. The static external failure pressure of the canister cover is studied via both theoretical and experimental approaches. A finite element model of the frangible cover is established and used for analyzing the stress distribution in the cover. The theoretical failure pressure of the canister cover is determined on the basis of the buckling or stress failure criteria. Static burst strength tests on a number of laminated composite canister covers were performed. Experimental results are used to validate the suitability of the design and verify the accuracy of the theoretical method for failure pressure prediction.

* Corresponding author. Tel.: +886-3-5725-634; fax: +886-3-5728-504.

E-mail address: tykam@cc.nctu.edu.tw (T.Y. Kam).

0263-8223/99/$ - see front matter © 2000 Elsevier Science Ltd. All rights reserved.
PII: S0263-8223(00)00022-2

2. Frangible laminated composite cover

The geometries of the previously proposed frangible laminated composite canister covers, namely, types CA and CB, are shown in Figs. 1 and 2, respectively. The covers (types CA and CB) are convex structures, which are fabricated with four plate-like laminated composite parts and a laminated composite frame. All the laminated composite components are adhesively bonded together along with their edges in forming the cover. The canister cover is designed in such a way that when subjected to an impulsive pressure, the adhesive bonds between the components will be broken and the severed plate-like laminated composite parts are blown away from the opening of the frame.

The laminated composite components of the canister cover are fabricated with two types of glass fabric/epoxy plies, namely, glass fabric A/epoxy and glass fabric B/epoxy. All the glass fabric/epoxy plies are balanced orthotropic materials for which the in-plane Young's moduli in material (fiber and matrix) directions, i.e., E_1 and E_2, are the same. The laminated composite components are fabricated in such a way that the stack of glass fabric B/epoxy plies is sandwiched in between those of glass fabric A/epoxy plies. The material properties of different cured glass fabric/epoxy plies are listed in Table 1. Referring to the lamina material directions, the stress–strain relations of a balanced orthotropic lamina can be expressed as

$$\begin{Bmatrix} \sigma_1 \\ \sigma_2 \\ \sigma_6 \end{Bmatrix} = \begin{bmatrix} Q_{11} & Q_{12} & 0 \\ Q_{12} & Q_{11} & 0 \\ 0 & 0 & Q_{66} \end{bmatrix} \begin{Bmatrix} \varepsilon_1 \\ \varepsilon_2 \\ \varepsilon_6 \end{Bmatrix}, \tag{1}$$

where σ_1, σ_2 are normal stresses, σ_6 is shear stress, $\varepsilon_1, \varepsilon_2$ normal strains, ε_6 is engineering shear strain. The components of the lamina stiffness matrix, Q_{ij}, are obtained as

$$Q_{11} = \frac{E_1}{1 - v_{12}^2}, \quad Q_{12} = \frac{v_{12}E_1}{1 - v_{12}^2}, \quad Q_{66} = G_{12}, \tag{2}$$

where v_{12} is the Poisson's ratio, G_{12} is the in-plane shear modulus. The in-plane stress–strain relations of a balanced orthotropic laminate are expressed as

$$\begin{Bmatrix} \overline{\sigma}_1 \\ \overline{\sigma}_2 \\ \overline{\sigma}_6 \end{Bmatrix} = \frac{1}{h} \begin{bmatrix} A_{11} & A_{12} & 0 \\ A_{12} & A_{11} & 0 \\ 0 & 0 & A_{66} \end{bmatrix} \begin{Bmatrix} \varepsilon_1 \\ \varepsilon_2 \\ \varepsilon_6 \end{Bmatrix}, \tag{3}$$

where $\overline{\sigma}_i$ are average stresses, h is laminate thickness. The components of the laminate stiffness matrix, A_{ij} are obtained as

$$A_{ij} = \int_{-\frac{h}{2}}^{\frac{h}{2}} Q_{ij}\, \mathrm{d}z, \quad i,j = 1,2,6. \tag{4}$$

By inversion, Eq. (3) can be rewritten as

$$\begin{Bmatrix} \varepsilon_1 \\ \varepsilon_2 \\ \varepsilon_6 \end{Bmatrix} = h \begin{bmatrix} a_{11} & a_{12} & 0 \\ a_{12} & a_{11} & 0 \\ 0 & 0 & a_{66} \end{bmatrix} \begin{Bmatrix} \overline{\sigma}_1 \\ \overline{\sigma}_2 \\ \overline{\sigma}_6 \end{Bmatrix}, \tag{5}$$

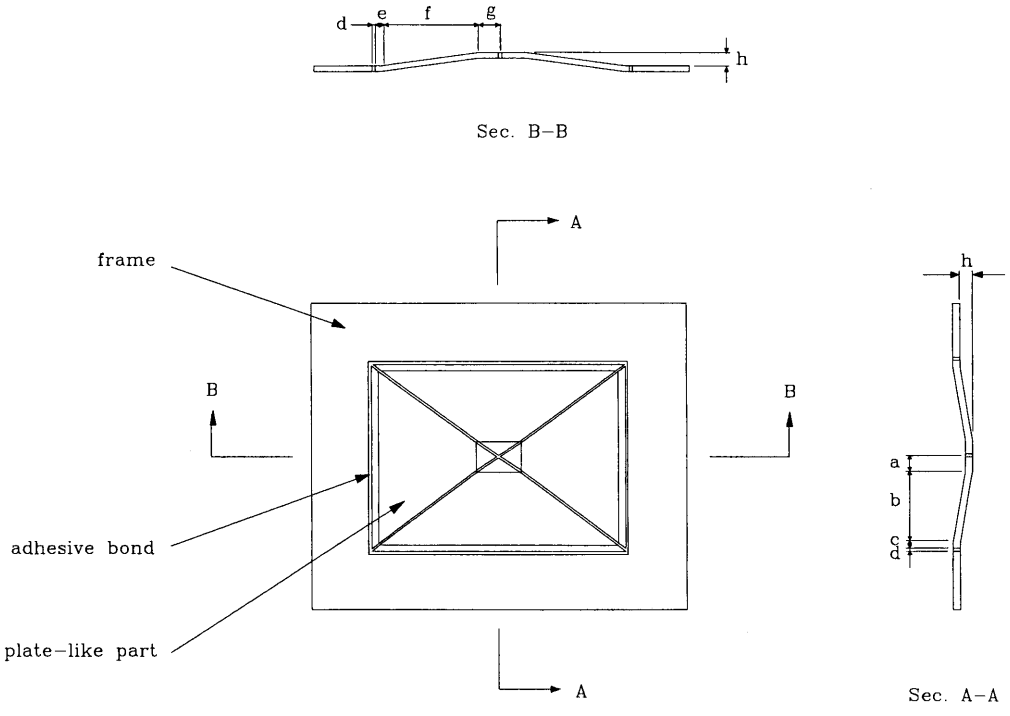

Fig. 1. Geometry of frangible canister cover CA.

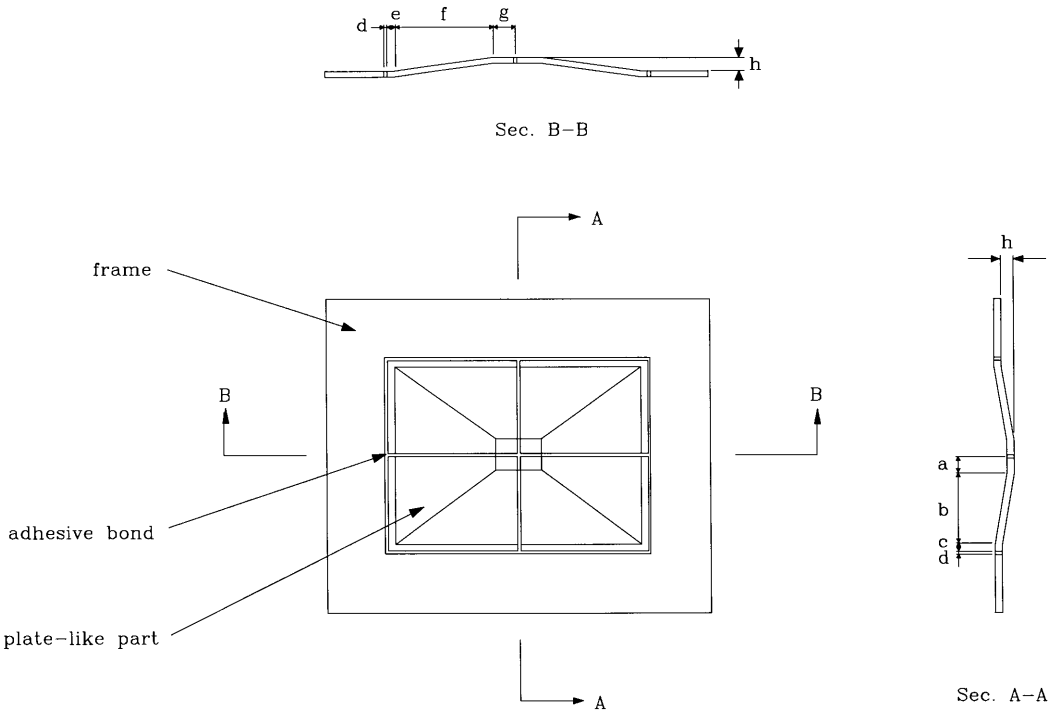

Fig. 2. Geometry of frangible canister cover CB.

Table 1
Properties of different composite laminae

Material type	Material constant[a]			Strength parameter[b]			Lamina thickness (mm)
	E_1 (GPa)	G_{12} (GPa)	v_{12}	X_T (MPa)	X_C (MPa)	S (MPa)	
Glass fabric A/epoxy	19.70	1.03	0.106	184.33	251.56	57.48	0.22
Glass fabric B/epoxy	24.95	2.00	0.143	369.00	504.03	44.91	0.44

[a] Coefficients of variation are about 5%.
[b] Coefficients of variation are about 8%.

where a_{ij} are the components of the laminate compliance matrix. Once a_{ij} are known, the effective engineering constants of the balanced orthotropic laminate can be obtained as

$$\overline{E}_1 = \frac{1}{a_{11}h}, \quad \overline{v}_{12} = -\frac{a_{12}}{a_{11}}, \quad \overline{G}_{12} = \frac{1}{a_{66}h}, \tag{6}$$

where $\overline{E}_1, \overline{v}_{12}, \overline{G}_{12}$ are the effective in-plane longitudinal Young's modulus, Poisson's ratio, and shear modulus, respectively.

3. Failure analysis of frangible cover

The finite element method formulated on the basis of the theory of linear elasticity is used to evaluate the stress distribution in and buckling strength of the composite canister cover. In order to include all possible buckling mode shapes, the full cover is considered in the finite element analysis. Since the width, d, of the adhesive bond is much smaller than its depth. It will be more appropriate to model using the adhesive bond in three-dimensional (3D) brick elements than in two-dimensional (2D) plate elements. Therefore, all the components of cover CA are modeled by eight-node brick and six-node wedge elements while those of cover CB by eight-node brick elements. When constructing the finite element mesh, a number of layers of elements are considered in the thickness directions of the components and the aspect ratios of the elements are chosen in such a way that no numerical instability occurs. The material constants for the elements of the laminated composite components are determined on the basis of the concept of effective engineering constants as mentioned in the previous section. Furthermore, since the length-to-thickness ratios of the laminated components are large, it is reasonable to assume that the stress in the thickness direction is negligible. For simplicity, it is assumed that the material constants in the thickness direction have the following properties

$$\overline{E}_3 = \overline{E}_1, \quad \overline{v}_{13} = \overline{v}_{12}, \quad \overline{G}_{13} = \overline{G}_{12}, \tag{7}$$

Table 2
Properties of different types of adhesive

Adhesive type	Material constant[a]			Strength parameter[b]	
	E (GPa)	G (GPa)	v	X_T (MPa)	S (MPa)
I	1.264	0.498	0.269	31.57	6.837
II	1.251	0.496	0.261	21.5	4.125
III	1.231	0.491	0.253	18.3	4.524
IV	1.157	0.464	0.247	12.4	4.860
V	2.152	0.784	0.373	35.7	11.68

[a] Coefficients of variation are about 5%.
[b] Coefficients of variation are about 10%.

where $\overline{E}_3, \overline{v}_{13}, \overline{G}_{13}$ are effective Young's modulus, Poisson's ratio, and transverse shear modulus in the thickness direction, respectively. On the other hand, the adhesive is assumed to be isotropic. Different types of adhesive have been used in bonding the cover components and their material properties are listed in Table 2.

In the failure analysis of the canister cover, two types of failure modes, namely, material failure and structural instability are considered. For the case of material failure, two phenomenological failure criteria, namely, the Tsai–Wu and maximum stress criteria are used to study the incipient failures in the components. In particular, the incipient failure in the laminated composite components is identified using the Tsai–Wu criterion [8].

$$F_{11}\sigma_1^2 + 2F_{12}\sigma_1\sigma_2 + F_{22}\sigma_2^2 + F_{66}\sigma_6^2 + F_1\sigma_1 + F_2\sigma_2 = 1 \quad (8)$$

with

$$F_1 = \frac{1}{X_T} - \frac{1}{X_C}, \qquad F_{12} = -\frac{1}{2\sqrt{X_T^2 X_C^2}},$$
$$F_2 = F_1, \qquad F_{66} = \frac{1}{S^2}, \quad (9)$$
$$F_{11} = \frac{1}{X_T X_C}, \qquad F_{22} = F_{11},$$

where X_T, X_C are the in-plane lamina tensile and compressive strengths in the fiber direction, respectively, S is the in-plane shear strength. It is noted that the actual stresses rather than the average stresses in each lamina of the laminated composite components are used in the above failure criterion for failure prediction. On the other hand, the incipient failure in the adhesive bonds is identified using the maximum stress failure criterion, which states that failure of the material is assumed to occur if any of the following conditions is satisfied

$$\sigma_{max} \geqslant X'_T \quad \text{or} \quad \tau_{max} \geqslant S', \quad (10)$$

where σ_{max}, τ_{max} are the maximum principal and shear stresses, respectively, X'_T, S' are adhesive tensile and shear strengths, respectively. It is noted that failure of an adhesive bond line is always induced by the maximum tensile stress developed in the adhesive. The value of the maximum shear stress is small and its effect on the failure of adhesive is minimal. Since the adhesive used in fabricating the frangible covers is brittle, it is thus appropriate to predict adhesive failure using the maximum stress criterion. For the case of structural instability, the buckling pressure is determined by solving the following eigenvalue problem.

$$KD = \lambda K_g D, \quad (11)$$

where K, K_g are structural stiffness and geometric stiffness matrices, D the vector of nodal displacements, λ is the buckling pressure.

4. Experimental investigation

A number of frangible laminated composite canister cover specimens were fabricated and subjected to external static pressure tests. The dimensions of the test specimens are listed in Table 3. The notation used for denoting the lay-up of a laminated composite component is $[A_n/B_m]_s$ where A and B denote the laminae of fabric A/epoxy and fabric B/epoxy, n and m numbers of plies, and s is symmetric lamination. A schematic description of the experimental setup for external static pressure test is shown in Fig. 3. The frame of the cover specimen under testing was properly clamped on the lug at one end of the cylindrical pressure tank while air was pumped into the tank from the other end. It is noted

Table 3
Dimensions of different cover specimens

Cover specimen	Dimensions (mm)							
	a	b	c	d	e	f	g	h
Small scale	10	50	5	1	5	65	15	8
Full scale	50	250	10	2	10	325	75	40

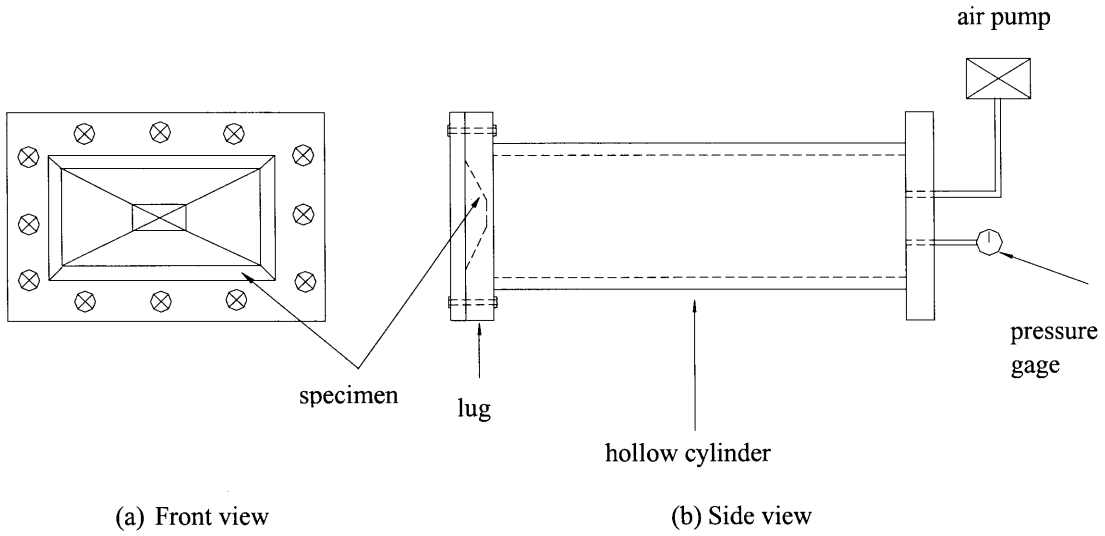

Fig. 3. Experimental setup for burst strength test.

that the convex side of the cover is facing toward the cylindrical pressure tank. The flow rate of the air pumped into the tank was slow enough that no excitation of the specimen was induced. The ultimate pressure that the specimen could sustain was measured via a pressure gauge attached to the tank. Visual inspection of the cover specimens, which had been tested and showed that failure always occurred at the adhesive bond lines between the plate-like parts and the rectangular frame. It is noted that since both buckling and material failure may lead to the same failure pattern of the frangible covers, the failure modes of the covers cannot be identified directly by pure visual inspection of the failed specimens.

Table 4
Convergence test of the finite element model for the full-scale $[A_2/B_5]_s$ cover CB

Mesh type	Number of nodes	Number of elements	Buckling pressure (kPa)
I	2489	2416	115.66
II	3217	3136	115.68
III	3952	4041	115.70

5. Results and discussion

The aforementioned methods for failure prediction are used to predict the external failure pressure of the frangible laminated composite canister covers that are to

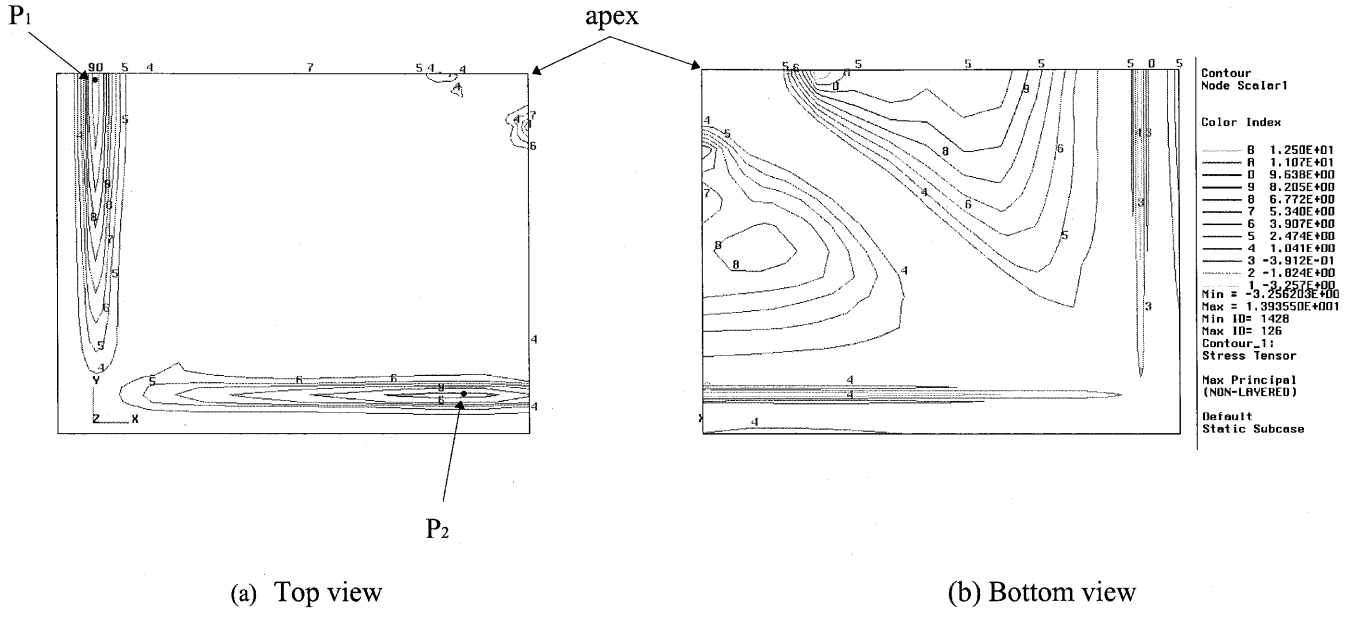

Fig. 4. Distribution of the maximum principal stress in $[A_2/B_2]_s$ quarter cover CA.

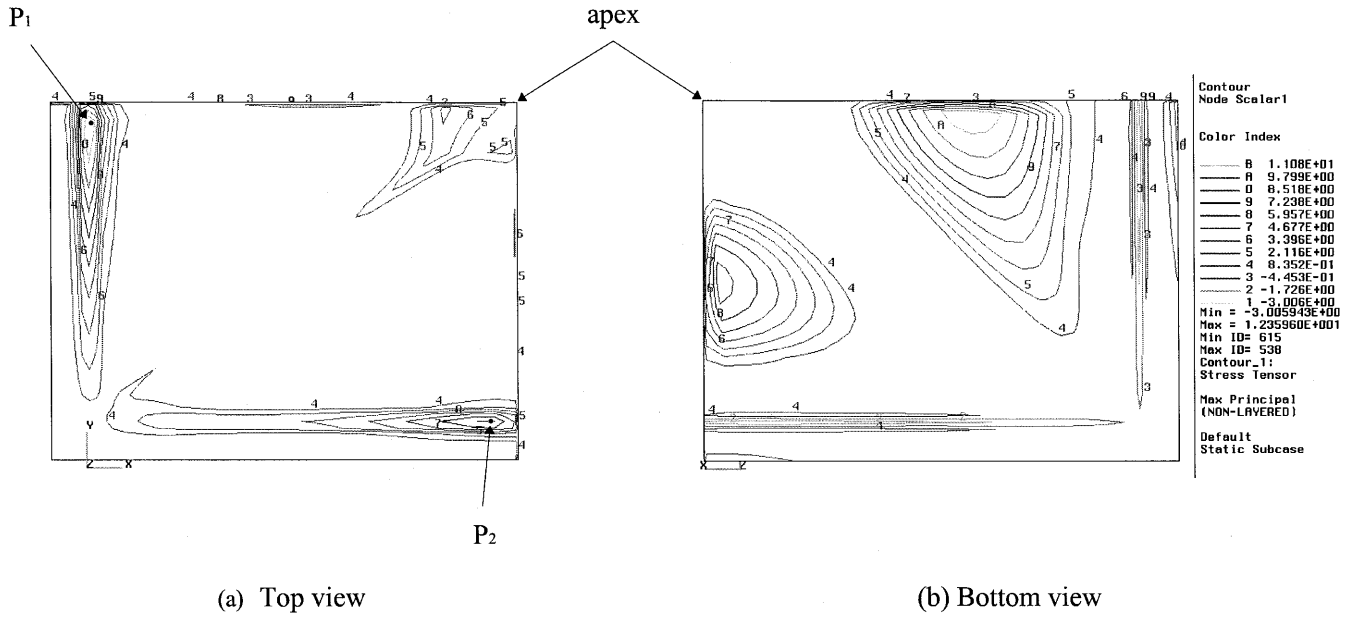

Fig. 5. Distribution of the maximum principal stress in $[A_2/B_2]_s$ quarter cover CB.

Table 5
External failure pressure of small-scale frangible canister covers

Cover specimen			External failure pressure (kPa)					Internal failure pressure (kPa)
Lay-up	Adhesive type	Cover type	Experimental (I)	Theoretical		Percentage difference		
				Buckling (II)	Material failure (III)	$\left\|\frac{I-II}{I}\right\| \times 100$	$\left\|\frac{I-III}{I}\right\| \times 100$	
$[A_2/B_2]_s$	II	CA	172.4	617.8	153.1	258.4	11.2	86.19
		CB	165.5	582.6	148.9	252.0	10.3	96.53
$[A_2/B_3]_s$	II	CA	>206.9	933.6	256.5	–	–	103.43
		CB	>206.9	862.6	253.7	–	–	110.32
	III	CA	>206.9	924.6	217.9	–	–	93.08
		CB	>206.9	857.7	212.4	–	–	93.08

Table 6
External failure pressure of full-scale frangible canister covers

Cover specimen			External failure pressure (kPa)			Percentage difference	
Lay-up	Adhesive type	Cover type	Experimental (I)	Theoretical		$\left\|\frac{I-II}{I}\right\| \times 100$	$\left\|\frac{I-III}{I}\right\| \times 100$
				Buckling (II)	Material failure (III)		
$[A_2/B_2]_s$	IV	CB	72.4	273.0	79.3	277.1	9.5
$[A_2/B_3]_s$	IV	CB	103.4	390.3	99.3	277.5	4.0

be tested. Herein the commercial finite element code NASTRAN [9] is used to perform the finite element analysis of the covers. All the laminated composite components and adhesive bond lines of the frangible covers are modeled by the aforementioned 3D elements. A convergence test of the finite element model for buckling analysis is first performed to determine the suitable finite element mesh. For illustration, the buckling pressure of the $[A_2/B_{10}]_s$ cover CB has been determined using different types of finite element mesh and the results are listed in Table 4. It is noted that the differences among the buckling pressures predicted by the various types of finite element mesh are small. For the sake of saving computing time, mesh type I will be adopted in the failure analyses of the other frangible covers. It's worth noting that the buckling mode associated with the buckling pressure is symmetric with respect to the planes of symmetry of the covers. The

maximum principal stress distributions of the quarter $[A_2/B_2]_s$ covers CA and CB (full-scale) subjected to external pressure of magnitude 68.95 kPa are shown in Figs. 4 and 5. If failure of frangible covers is predicted on the basis of the maximum stress criterion then it is obvious that points P1 and P2 in the adhesive bond lines between the rectangular frame and the plate-like parts are likely to be the locations, where incipient failure will be incurred in the frangible cover. The theoretically predicted failure locations of the cover specimens seem to conform with those observed experimentally. Based on different failure criteria, the theoretical failure pressures of various frangible cover specimens are computed and the results listed in Tables 5 and 6 in comparisons with the experimental results. In Table 5, the experimental failure pressures of the $[A_2/B_3]_s$ covers CA and CB exceed 206.9 kPa at which the tests were terminated. In view of the results in Tables 5 and 6, it is obvious that the failure mode of the covers is material failure and the theoretical method can produce reasonable predictions of the failure pressure of the covers. The errors in the theoretical predictions of the failure pressure based on the material failure criterion can be attributed to the existence of uncertainty in the material properties. It is also noted that the covers with same size, cover CA is generally stronger than cover CB. The thickness of the bond lines, i.e., the thickness of the laminated components has important effects on the failure pressure of the covers. The increase in the thickness of the bond lines can raise the failure pressure of the covers. A comparison between the external and internal failure pressures of the small-scale covers is also performed. As indicated by the results listed in Table 5, it is obvious that the external failure pressure of the covers is much higher than their internal failure pressure.

6. Conclusions

The external failure pressures of two new frangible laminated composite canister covers were studied via both theoretical and experimental approaches. The failure mode of the frangible covers under external pressure was identified to be material failure. Good agreements between the theoretical and experimental results were observed. The thickness of the bond lines between the rectangular frame and the plate-like parts of the covers had important effects on the failure pressure of the covers. It was also shown that different types of cover designs (CA or CB) could have different external pressure resistance. It is recommended that both external and internal pressure resistance of a frangible cover be considered simultaneously if a proper design of the cover is to be pursued.

Acknowledgements

This research was supported by the National Science Council of the Republic of China under grant No. NSC 86-2623-D-009-008. Their support is gratefully acknowledged.

References

[1] Bell RE. Missile weapon system. US Patent No. 5239909, 1992.
[2] Boeglin PH. Plate-glass fitted with an explosion-cutting device. US Patent No. 4333381, 1982.
[3] Mussey RA. Launch tube closure. US Patent No. 4301708, 1981.
[4] Copeland RL, Greene RF. Protective cover for a missile nose cone. US Patent No. 3970006, 1976.
[5] Krol UB. Frangible cover assembly for missile launchers. US Patent No. 3742814, 1971.
[6] Doane WJ. Frangible fly through diaphragm for missile launch canister. US Patent No. 4498368, 1985.
[7] Wu JH, Wang WT, Kam TY. Failure analysis of a frangible laminated composite canister cover. In: Proc Inst Mech Eng, vol. 213, Part G, 1999, p. 187–95.
[8] Tsai SW, Hahn HT. Introduction to composite materials. Westport, Connecticut: Technomic Publishing Company, 1980.
[9] Caffrey JP, Lee JM. MSC/NASTRAN linear static analysis user's guide version 68. Los Angeles, USA: The Macneal-Schwendler Corporation, 1994.